

A Well-defined Hierarchical Hydrogen Bonding Strategy to Polyureas with Simultaneously Improved Strength and Toughness

Li Ting, Zheng Tian-Ze, Guo Zhao-Xia, Xu Jun, Guo Bao-Hua

Cite this article as:

Li Ting, Zheng Tian-Ze, Guo Zhao-Xia, Xu Jun, Guo Bao-Hua. A Well-defined Hierarchical Hydrogen Bonding Strategy to Polyureas with Simultaneously Improved Strength and Toughness[J]. *Chinese J. Polym. Sci.*, 2019, 37(12): 1257-1266. doi: 10.1007/s10118-019-2275-3

View online: <https://doi.org/10.1007/s10118-019-2275-3>

Articles you may be interested in

SYNTHESIS AND CHARACTERIZATION OF WELL-DEFINED BLOCK COPOLYMERS CONTAINING PENDANT, SELF-COMPLEMENTARY QUADRUPLE HYDROGEN BONDING SITES

Chinese J. Polym. Sci. 2008, 26(6): 767

Synthesis of Well-defined Telechelic Trans-1,4-polyisoprene by Oxidative Cleavage

Chinese J. Polym. Sci. 2016, 34(3): 359 <https://doi.org/10.1007/s10118-016-1746-z>

IMPROVED OXYGEN PERMEABILITY AND MECHANICAL STRENGTH OF SILICONE HYDROGELS WITH INTERPENETRATING NETWORK STRUCTURE

Chinese J. Polym. Sci. 2010, 28(6): 849 <https://doi.org/10.1007/s10118-010-9142-6>

完全交替结构乙烯-丙烯共聚物的制备与表征

SYNTHESIS AND CHARACTERIZATION OF WELL-DEFINED ALTERNATING ETHYLENE-PROPYLENE COPOLYMER

高分子学报. 2010(8): 941 <https://doi.org/10.3724/SP.J.1105.2010.10105>

特定结构的卟啉聚合物的构建及应用

Construction and Applications of Well-defined Porphyrin-containing Polymers

高分子学报. 2019, 50(7): 653 <https://doi.org/10.11777/j.issn1000-3304.2019.19018>

具有明确硬段结构的水性聚氨酯脲的研究

STUDIES OF A WELL-DEFINED MODEL HARD SEGMENT AND WATERBORNE POLYURETHANEUREA

高分子学报. 2006(3): 461

A Well-defined Hierarchical Hydrogen Bonding Strategy to Polyureas with Simultaneously Improved Strength and Toughness

Ting Li, Tian-Ze Zheng, Zhao-Xia Guo, Jun Xu*, and Bao-Hua Guo*

Key Laboratory of Advanced Materials (Ministry of Education), Department of Chemical Engineering, Tsinghua University, Beijing 100084, China

 Electronic Supplementary Information

Abstract A well-defined quadruple hydrogen bonding strategy involving dimerization of 2-ureido-4[1*H*]-pyrimidone (UPy) units is innovatively designed to prepare polyureas with high overall mechanical properties. Three polyureas containing different amounts of UPy units were synthesized by replacing a portion of isophorone diisocyanate (IPDI) with a UPy-derived diisocyanate. The formation of quadruple hydrogen bonds in hard segments *via* UPy dimers was confirmed by nuclear magnetic resonance (NMR) and Fourier transform infrared spectroscopy (FTIR). The mechanical properties of the polyureas were evaluated by uniaxial tensile testing. Compared to the polyurea without UPy units, remarkable improvements in Young's modulus, tensile strength, and toughness were simultaneously achieved when UPy units were incorporated. The mechanism behind the strong strengthening effect rooted in the stronger intermolecular forces among hard segments brought by the quadruple hydrogen bonds, which were stronger than the inherent bidentate and monodentate hydrogen bonds among urea groups, and the slower soft segmental dynamics revealed by both increased T_g and relaxation time of the soft segments. The mechanism behind the strong toughening effect was ascribed to more effective energy dissipation brought by the quadruple hydrogen bonds that served as stronger sacrificial bonds upon deformation. This work may offer new insight into the design of polyurea elastomers with comprehensively improved mechanical properties.

Keywords Mechanical properties; Strength; Toughness; Quadruple H-bonds; Polyurea elastomers

Citation: Li, T.; Zheng, T. Z.; Guo, Z. X.; Xu, J.; Guo, B. H. A well-defined hierarchical hydrogen bonding strategy to polyureas with simultaneously improved strength and toughness. *Chinese J. Polym. Sci.* 2019, 37, 1257–1266.

INTRODUCTION

Polyurea elastomers are a type of versatile materials that find a wide range of commercial applications in the field of coatings for anticorrosion protection of concrete,^[1] parking decks, freight ships, bridges,^[2–5] *etc.* They are segmented block copolymers with typical phase-separated micro-structures: hard segments comprising isocyanates and amine chain extenders self-assemble *via* intermolecular interactions (mainly hydrogen bonding) into hard domains embedded in a continuous matrix of flexible soft segments^[6,7] generated by long chain diamines (*e.g.* polyether, polyester, and PDMS based diamines).^[5,8] The hard domains act as physical crosslinks,^[9] giving rise to practicable mechanical properties. However, for some applications, such as protective coatings for military armors to resist the speeding shrapnels,^[10] excellent mechanical properties including Young's modulus, tensile strength, and even toughness are urgently required. Therefore, improving the mechanical properties of polyureas is an important topic of research.

There are two strategies that are commonly used for improving mechanical properties of polyureas. One is to incorporate nanofillers,^[11–15] and the other is to increase chemical cross-links.^[16] Both methods can significantly improve the Young's modulus and tensile strength of polyureas. However, the preparation of nano-fillers is complicated due to the necessity of surface modification to solve the dispersion problem,^[11,12] and chemical crosslinks increase elastomer's stiffness at the sacrifice of extensibility.^[16] These drawbacks strongly motivate us to exploit new ways to simultaneously improve the strength, stiffness, and toughness of polyurea elastomers.

Hydrogen bonding between the urea linkage plays an essential role in the formation of hard domains^[17,18] and makes important contribution to the mechanical properties of polyureas.^[19,20] Our research group and other researchers have demonstrated that, when hydrogen bonds in hard domains were disrupted by heating^[5] or hydrogen bond dissociation agents (*e.g.* lithium halides),^[21,22] Young's modulus and tensile strength would decline. It is reasonable to infer that the Young's modulus and tensile strength will increase if hierarchical hydrogen bonding, which is stronger than the inherent bidentate or monodentate hydrogen bonding among urea groups,^[5,23] is introduced into the hard domains.

* Corresponding authors: E-mail jun-xu@mail.tsinghua.edu.cn (J.X.)
E-mail bhguo@mail.tsinghua.edu.cn (B.H.G.)

Received March 16, 2019; Accepted April 15, 2019; Published online June 13, 2019

2-Ureido-4[1*H*]-pyrimidone (UPy) unit is well-known for its dimerization through the formation of well-defined quadruple hydrogen bonds.^[24–26] It has been widely explored in the field of supramolecular chemistry for the synthesis of high-molecular-weight and dynamic supramolecular polymers^[24–26] due to its high dimerization constant ($> 10^7$ L/mol in chloroform).^[27–30] The high bonding energy ($\Delta G \approx 40$ kJ/mol) of UPy dimers and the reversible property of hydrogen bonds have been taken advantages for improving a specific property of some polymers, such as the toughness of polyisoprene and the self-healing property of polyurethanes. For example, Luo *et al.*^[31,32] introduced UPy units into side chains of polyisoprene to increase additional crosslinks and found that both the toughness and tensile strength were remarkably enhanced because the quadruple hydrogen bonds can serve as sacrificial bonds^[33] to dissipate energy and redistribute stress. Considering the essential role of hard domains acting as physical crosslinks in polyureas^[5] and the efficiency of quadruple hydrogen bonds in energy dissipation, it is very likely to realize simultaneous strengthening and toughening of polyureas by incorporating UPy units.

In the present work, we innovatively introduce UPy units into hard domains of a polyurea elastomer by partially replacing the classical diisocyanate (isophorone diisocyanate, IPDI) with UPy-derived diisocyanates (NCO-UPy-NCO) for the purpose of affording polyureas with simultaneously improved strength, stiffness, and toughness through formation of well-defined quadruple hydrogen bonds. The formation of quadruple hydrogen bonds is confirmed by nuclear magnetic resonance (NMR) and Fourier transform infrared spectroscopy (FTIR). Both strengthening and toughening mechanisms are investigated.

EXPERIMENTAL

Materials

Diaminopolypropylene glycol (Jeffamine[®] D2000, $M_w = 2000$) was purchased from Huntsman International LLC. Dimethyl thio-toluene diamine (DMTDA) was purchased from Aladdin. D2000 and DMTDA were dried under vacuum at 90 °C for 5 h. Isophorone diisocyanate (IPDI, 99%), 2-acetyl butyrolactone, and guanidine carbonate were bought from Energy Chemical and used as received. All the solvents were dried before use.

Sample Preparation

Preparation of (2-amino-5-(2-hydroxyethyl)-6-methylpyrimidin-4-ol) (HO-UPy-NH₂)
HO-UPy-NH₂ (Fig. S1 in electronic supplementary information, ESI) was synthesized according to the literature as follows.^[26] 2-Acetyl butyrolactone (6 mL) and guanidine carbonate (9.9 g) were stirred in absolute ethanol (60 mL). The mixture was refluxed overnight in the presence of triethylamine (15.6 mL). The suspension liquid was yellow and turbid. After cooling, aqueous HCl was used to adjust the pH to 6–7. After filtration, the solid was extensively washed with ethanol and dried. ¹H-NMR (Fig. S3 in ESI, 600 MHz, DMSO-*d*₆, δ , ppm): 11.0 (aH, —N—H), 6.5 (bH, —NH₂), 4.5 (fH, —O—H), 3.4 (cH, —CH₂ of —CH₂—OH), 2.4 (dH,

—CH₂ of —CH₂—CH), 2.1 (eH, —CH₃).

Preparation of UPy-isophorone-diisocyanate (NCO-UPy-NCO)

2-Amino-5-(2-hydroxyethyl)-6-methylpyrimidin-4-ol (UPy, 0.8 g) and isophorone diisocyanate (IPDI, 10 mL) were added into a three-necked flask and stirred at 90 °C under nitrogen. After 24 h, the solution was precipitated into hexane (500 mL) and then stirred under nitrogen. A white solid was isolated by filtration. ¹H-NMR (Fig. S4 in ESI, 600 MHz, CDCl₃, δ , ppm): 12.9 (aH, —N—H—), 12.0–11.9 (bH, —N—H— of UPy), 10.2 (cH, —N—H— of urea bonds), 4.2 (fH, —CH₂ of —CH₂—OH), 2.6 (eH, —CH₂ of UPy), 2.2 (dH, —CH₃ of UPy). Note: There are two isomers (*cis* and *trans*) in IPDI that may react at the different isocyanate positions, resulting in a mixture of 16 isomers for NCO-UPy-NCO.

*Synthesis of polyurea PU-*x*UPy elastomers*

The polyureas are denoted as PU-*x*UPy, where *x* means the molar percentage of NCO-UPy-NCO in all the diisocyanates (*x* = 0, 1/6, 1/3). Our target polyureas were synthesized by the reaction between diaminopolypropylene glycol (D2000) and a mixture of isophorone diisocyanate (IPDI) and NCO-UPy-NCO with dimethyl thio-toluene diamine (DMTDA) as the chain extender. The synthetic procedure of PU-*x*UPy samples is illustrated in Scheme 1.

The typical procedure for the synthesis of PU-1/6UPy is as follows. Firstly, IPDI (0.50 g, 2.25 mmol), NCO-UPy-NCO (0.28 g, 0.45 mmol), D2000 (2.16 g, 1.08 mmol), and DMTDA (0.35 g, 1.62 mmol) were separately dissolved in chloroform (0.5 g/mL) in different beakers. Secondly, the mixture of IPDI and NCO-UPy-NCO solutions was transferred into a 100 mL three-necked flask with a magnetic stir bar. D2000 solution was dropwise added into the three-necked flask with a constant pressure drop funnel. The mixture was stirred at room temperature for 30 min to give an isocyanate terminated prepolymer. Thirdly, DMTDA solution was added into the system, which acted as the chain extender. The system was then kept stirring and monitored by FTIR spectroscopy until the disappearance of isocyanate band around 2270 cm⁻¹. All the procedures were conducted under N₂ atmosphere to avoid any side reactions. Finally, the solution was poured into a Teflon mold at room temperature, held for 24 h to evaporate the solvent, and then further dried at 80 °C under vacuum for 12 h to ensure a complete reaction and solvent volatilization.

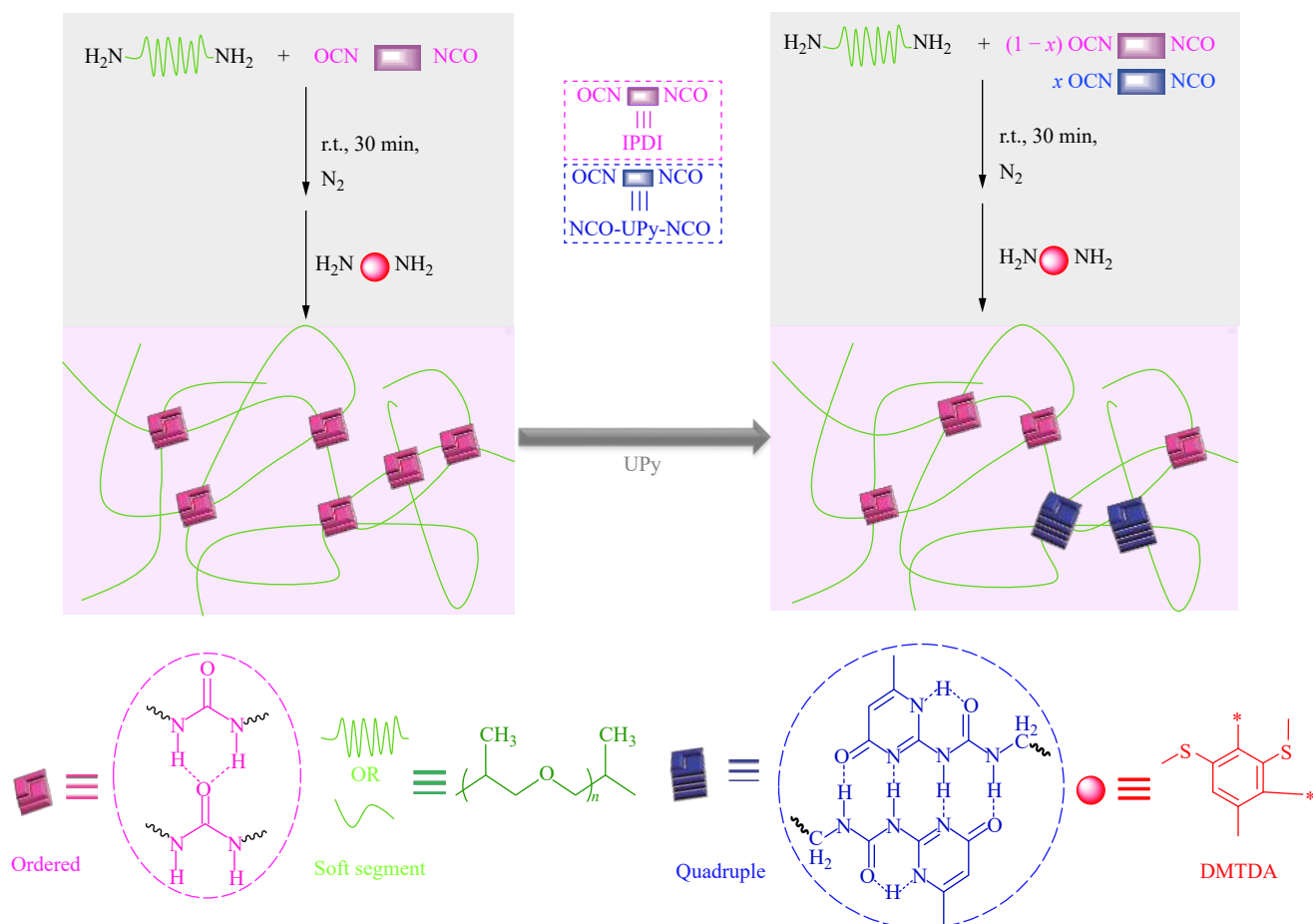
Characterization

Nuclear magnetic resonance (NMR) and Fourier transform infrared spectroscopy (FTIR)

¹H-NMR spectra were recorded on a JEOL ECS-400 instrument with CDCl₃ and DMSO-*d*₆ as the solvents using tetramethylsilane as an internal reference. The FTIR spectra were recorded with a Nicolet 6700 infrared spectrophotometer over 600–4000 cm⁻¹ with a 2 cm⁻¹ resolution. Measurements were performed after solvent evaporation on a KBr plate.

Mechanical evaluation

Dumbbell-shaped specimens were punched out of the samples according to GB/T-528. Stress-strain tests were carried out on a tensile test machine (SHIMADZU AGS/X, Japan)



Scheme 1 Synthetic routes and schematic illustration of polyureas without and with UPy (x means the molar percentage of NCO-UPy-NCO in total diisocyanates.)

at ambient conditions and a crosshead speed of 50 mm/min. Gradient tensile tests were carried out with a particular axial strain, then unloaded to zero stress, and reloaded with a higher axial strain, and so forth. Load-unload cyclic tensile tests were carried till the strain reached 50%, which was then set back to zero stress.

Dynamic mechanical analysis (DMA)

The rectangular sheets (about 30 mm × 8 mm × 2 mm) were cut from the samples, and DMA measurements were performed on an Anton Paar MCR301. The samples were tested on a stress/strain controlled rheometer in the torsional mode with a strain of 0.01% and a frequency of 1 Hz. Samples were cooled by liquid nitrogen to -90 °C, held at this temperature for 5 min, and heated to 200 °C at a heating rate of 4 °C/min.

Differential scanning calorimetry (DSC) tests

To examine the glass transition temperatures of different samples, a differential calorimeter (DSC-60, SHIMADZU) was used. Samples were heated from -90 °C to 230 °C with a heating rate of 20 °C/min and a nitrogen flow rate of 50 mL/min. The soft phase T_g was obtained from the first heating scan curve.

Broadband dielectric spectrometry (BDS)

To study the segmental dynamics of soft segments, dielectric spectroscopy measurements were carried out on a broadband

dielectric spectrometer (Alpha-T, Novocontrol Technologies GmbH & Co. KG) over a frequency range of 10^{-2} – 10^6 Hz. All samples with the thickness of *ca.* 0.15 mm were gold plated and placed between two parallel brass electrodes with a diameter of 10 mm. Relaxation spectra were measured under nitrogen with a temperature ranging from -70 °C to 10 °C.

Dielectric strength ($\Delta\epsilon$) and characteristic relaxation time (τ_{NH}) were obtained from Havriliak and Negami (HN) empirical equation^[34] as below:

$$\epsilon^*(\omega) = \epsilon_\infty + \frac{\Delta\epsilon}{(1 + (i\omega\tau_{\text{NH}})^\alpha)^\beta} \quad (1)$$

Here, ω is the angular frequency; $\Delta\epsilon = \epsilon_0 - \epsilon_\infty$ is the dielectric strength; ϵ_0 and ϵ_∞ are the relaxed and unrelaxed dielectric strength, respectively. α and β are shape parameters of the loss peak ($0 < \alpha, 0 < \alpha\beta < 1$), which are the overall symmetric distribution index and the asymmetric distribution index of the high frequency, respectively. τ_{NH} is related with τ_{max} as follows:

$$\tau_{\text{max}} = \frac{1}{2\pi f_{\text{max}}} = \tau_{\text{HN}} \left[\frac{\sin(\alpha\beta\pi/(2+2\beta))}{\sin(\alpha\pi/(2+2\beta))} \right]^{1/\alpha} \quad (2)$$

Here, f_{max} is the frequency where ϵ'' passes through the maximum value. f_{max} of α processes can be correlated with

the temperature following a Vogel-Fulcher-Tammann (VFT) form:

$$f_{\max} = f_0 \exp\left(\frac{B}{T - T_0}\right) \quad (3)$$

where T_0 is the Vogel temperature and the temperature coefficient (B) is an empirical parameter.

RESULTS AND DISCUSSION

Synthesis of Polyureas

UPy moiety could be introduced into the hard segments in two forms, either chain extender or diisocyanate. Although HO-UPy-NH₂ (Fig. S1, in ESI) could serve as a UPy-type chain extender, its poor solubility in low boiling point solvents^[30] led to low synthesis efficiency. In contrast, OCN-UPy-NCO synthesized by reacting HO-UPy-NH₂ with an excess amount of isophorone diisocyanate (IPDI) (Fig. S2, in ESI) showed excellent solubility in low boiling point solvents such as chloroform. Thus, UPy units were incorporated into the main chain of polyureas by replacing some IPDI with OCN-UPy-NCO. Polyureas containing 0, 1/6, and 1/3 molar fraction of OCN-UPy-NCO were straightforwardly synthesized using commercially available diaminopolypropylene glycol (Jeffamine® D2000) with CH₃ side groups as the soft constituent and commercial dimethyl thio-toluene diamine (DMTDA) as the chain extender, as shown in Scheme 1. Because the primary objective of introducing UPy moiety is to improve mechanical properties through formation of quadruple hydrogen bonds *via* dimerization of UPy units, proper solvent should be selected for the synthesis of polyureas when considering the dependency of UPy dimerization constant on the solvent polarity. Meijer *et al.*^[35] have reported that UPy existed in different states in different solvents. In less polar solvents such as CHCl₃, UPy units could easily assemble into dimers *via* DDAA and DADA array due to the high dimerization constants. On the contrary, UPy existed in the monomeric form in a polar aprotic solvent such as DMSO.^[35] Thus, we adopted chloroform as the solvent to prepare polyurea elastomers to ensure the formation of UPy dimers.

The existence of UPy dimers in the two polyureas containing UPy units was evidenced by comparing ¹H-NMR spectra of the same polyurea in two different solvents with different polarities. Fig. 1 shows the ¹H-NMR spectra of PU-1/3UPy in CDCl₃ and DMSO-d₆. In CDCl₃, the signals at $\delta = 13.3$, 11.9, and 10.1 ppm are ascribed to dimerized-UPy groups,^[35] similar to the case of NCO-UPy-NCO shown in Fig. S3 (in ESI). However, the signals shifted to upfield in DMSO-d₆, where typical signals of the intramolecular hydrogen-bonded pyrimidone N-H group ($\delta = 11.4$) and the non-hydrogen bonded ureido N-H group ($\delta = 9.4$ ppm) are assigned to the monomeric formation of UPy units, similar to the previous reports.^[36,37] These phenomena confirmed that UPy units could assemble into dimers *via* quadruple hydrogen bonds in chloroform. Since our polyureas were synthesized with chloroform as the solvent, well-defined quadruple hydrogen bonds were certainly formed in our polyureas with UPy units.

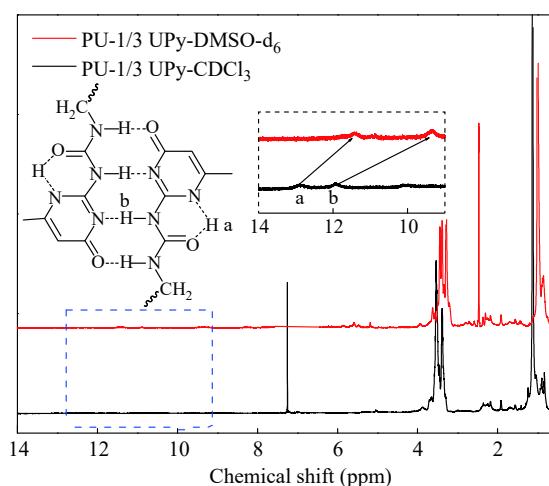


Fig. 1 ¹H-NMR spectra of PU-1/3UPy in CDCl₃ and DMSO-d₆

Fourier transform infrared spectroscopy (FTIR), which is a simple yet very effective technique to measure hydrogen bonding behavior,^[38] was applied to determine different types of hydrogen bonds in the three polyureas with or without UPy units by observing the spectral change of carbonyl (C=O) groups at 1640–1760 cm⁻¹ in Fig. 2(a). Generally, there are three kinds of carbonyl groups in a typical polyurea^[23] (Fig. 2b) from curve fitting in Fig. S6 (in ESI): “free” ones without hydrogen bonding (~1715 cm⁻¹), “disordered” ones with a single ligand hydrogen bond shifting to lower

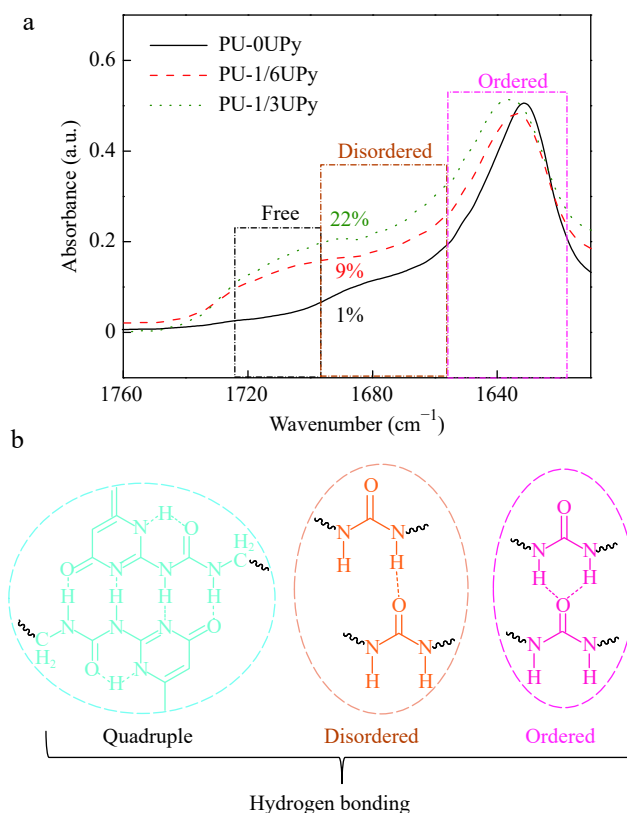


Fig. 2 (a) FTIR spectra for C=O groups of the three samples: PU-0UPy, PU-1/6UPy, and PU-1/3UPy; (b) Three typical hydrogen bonds in polyureas

wavenumber ($\sim 1680\text{ cm}^{-1}$), and “ordered” ones with a bidentate ligand at the lowest wavenumber ($\sim 1636\text{ cm}^{-1}$). Once UPy groups were incorporated into the hard segments of polyureas and form dimers, different kinds of hydrogen bonds would emerge (Fig. 2b), *i.e.* quadruple hydrogen bonds in UPy dimers, while there are little hydrogen bonds associated with carbonyl bonds in monomeric form of UPy units.^[36]

FTIR spectra of carbonyl groups for the three polyureas are normalized and presented in Fig. 2(a), where the intensity of “disordered” (*i.e.* monodentate) band becomes larger with increasing UPy content. This is reasonable, because the quadruple hydrogen bonds in UPy dimers mainly existed in the form of single ligand as shown in Fig. 2(b). The quantitative analysis was also performed to reveal the changes of hydrogen bonds. Date fitting clarified the area under the bands of three carbonyl bonds, and their corresponding percentage could be calculated as follows, assuming that the absorption coefficient of carbonyl bonds was 1.0.^[5,39,40]

$$X_d = \frac{A_d}{A_f + A_d + A_o} \quad (4)$$

where A_o , A_d , and A_f are the band areas of “ordered”, “disordered”, and “free” carbonyl groups, respectively. X_d is the percentage of “disordered” carbonyl groups. The values of X_d are given in the FTIR spectra in Fig. 2(a). The increasing “disordered” bonds (from 1% to 22%) with the

UPy content verified the existence of UPy dimers rather than monomeric forms.

Mechanical Properties of Polyureas

Mechanical properties of the three polyureas with or without UPy units were evaluated by static uniaxial tensile testing. Typical stress-strain curves are shown in Fig. 3(a), and the average values of Young’s modulus, tensile strength, and toughness are summarized in Figs. 3(b)–3(d). As shown in Fig. 3(a), the three polyureas exhibited similar stress-strain behavior with marked differences in modulus, strength and toughness.

Compared to the polyurea without UPy units, significant improvements in Young’s modulus, tensile strength, and toughness were simultaneously achieved when UPy units were incorporated (Figs. 3b–3d). Young’s modulus and tensile strength increased with increasing UPy content (Figs. 3b and 3c). When only 1/6 of IPDI was replaced by NCO-UPy-NCO, Young’s modulus and tensile strength were *ca.* 3.5 times and *ca.* 3 times of those of the polyurea without UPy, showing strong strengthening effect. Because hard domains act as reinforcing fillers in polyureas^[41] and the stronger intermolecular forces among hard segments brought by the stronger quadruple hydrogen bonds resulting from dimerization of UPy units make the “fillers” more rigid, the remarkable increases in modulus and strength are fully understandable from the aspect of rigid filler reinforcement. The poly-

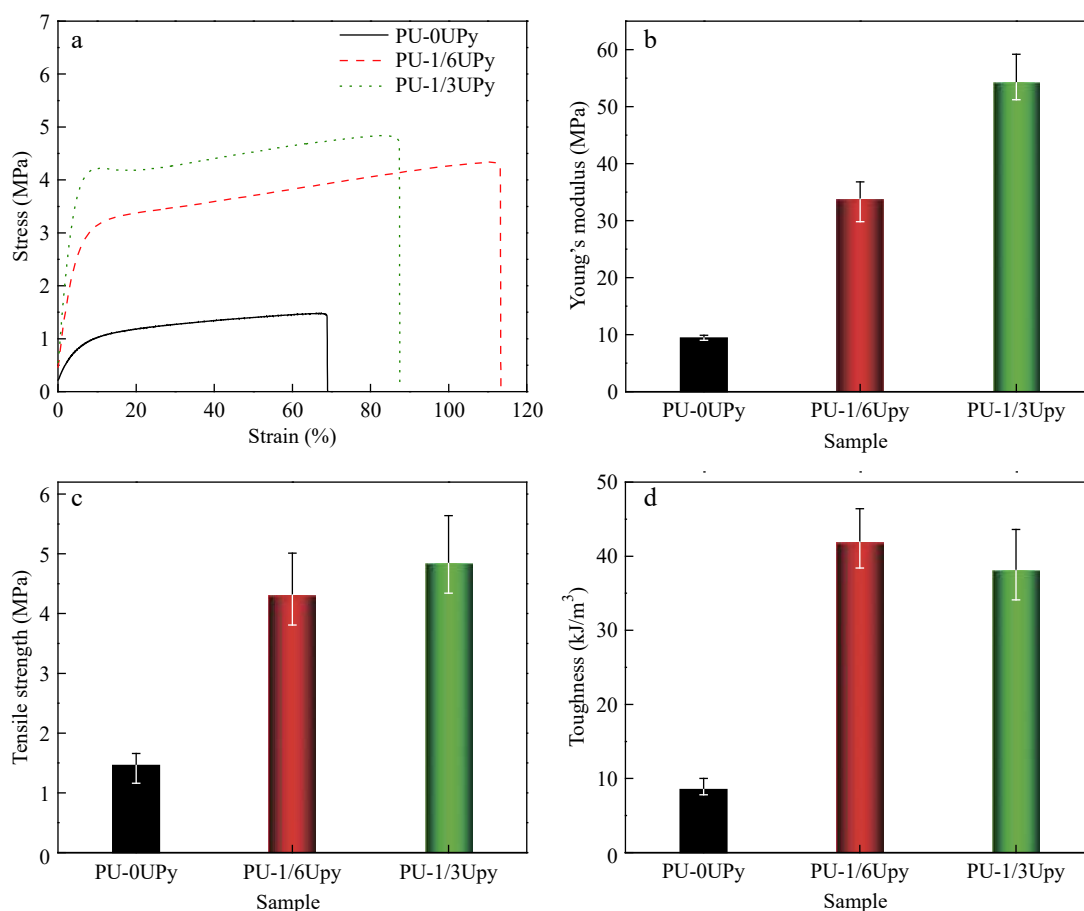


Fig. 3 (a) Stress-strain curves, (b) Young’s modulus, (c) tensile strength, and (d) toughness of three polyureas

urea PU-1/6UPy had the greatest toughness (Fig. 3d), which is *ca.* 4 times higher than that of the control sample PU-0UPy, ascribed to more efficient energy dissipation brought by the sacrificial quadruple hydrogen bonds, which will be discussed in next section.

Dynamic mechanical analysis was also carried out to evaluate the mechanical properties of the three polyureas. Temperature-dependent storage moduli are presented in Fig. 4. The storage modulus in the rubbery plateau region at -25 – 75 °C increased significantly with increasing UPy mole fraction, further confirming the stiffening effect of UPy units that resulted in stronger intermolecular forces in hard domains.

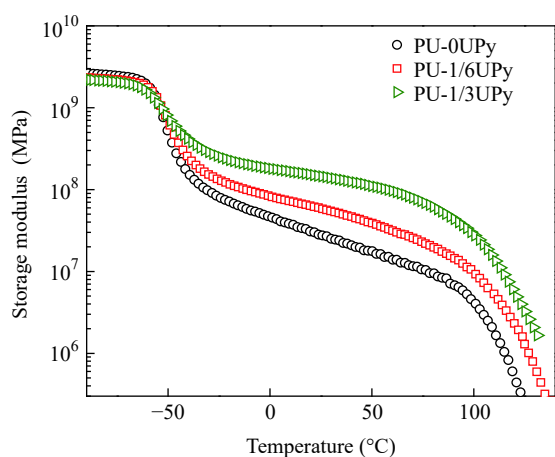


Fig. 4 Temperature dependence of storage modulus for the three samples

Effect of UPy Units on Energy Dissipation

It is known that noncovalent sacrificial bonds in polymers can efficiently dissipate energy through reversible bond rupture and therefore result in high toughness of polymers.^[42] To investigate the energy dissipation in our polyureas, cyclic tensile testing was performed using polyurea PU-1/6UPy as a representative. The sample was stretched to 50% strain, then back to 0% stress, and then a second load-unload cycle was performed. The cyclic stress-strain curves are presented in Fig. 5. Large hysteresis loop can be observed in the first cycle; the hysteresis loop decreases during the second cycle along with a softening behavior. These phenomena are similar to the Mullins effect of conventional rubber,^[3] implying that the breakdown of “crosslinks” governs the large dissipation of the first cycle and the “crosslinks” cannot “heal” themselves before the next cycle.^[5,6] The instantaneous permanent set can also be clearly observed due to the incomplete recovery of the microstructure. Here, the “crosslinks” refer to the hard domains in polyurea acting as physical crosslinks. Given that the formation of physical crosslinks is closely related to the hydrogen bonds, the breakage of hydrogen bonds is an essential factor for energy dissipation and contributes to toughness of the materials.^[31]

It has been proposed that the bond energies of hydrogen bonds (*ca.* 5–25 kJ/mol)^[35,43] are much lower than those of covalent bonds such as 350 kJ/mol for the C–C covalent bond. Thus, hydrogen bonds can be utilized as sacrificial

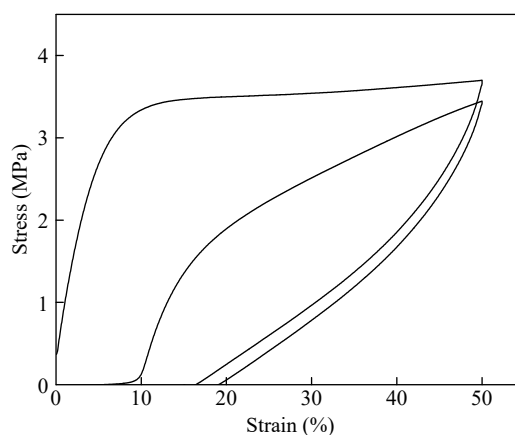


Fig. 5 Mechanical hysteresis behavior of PU-1/6UPy

bonds that preferentially break upon deformation to dissipate energy. More energy is required to break the quadruple hydrogen bonds than the bidentate or monodentate hydrogen bonds in a polyurea without UPy units. To further investigate the role of quadruple hydrogen bonds in energy dissipation, incremental loading and unloading cycles of the three polyureas were performed, and the curves are presented in Figs. 6(a)–6(c). In consistent with the cyclic tests in Fig. 5, softening behavior and residual strain are observed in each sample during the load-unload tensile tests; the instantaneous permanent set increases with increasing imposed strain. These data also reveal that the continuous breakup of physical crosslinks, which is associated with breakup of the hydrogen bonds shown in Fig. 6(d), contributes to the hysteresis loop. If we compare the three samples on one cycle during five successive loading-unloading cycles, for example the fifth cycles of these samples, the larger hysteresis areas with increasing UPy content are observed, implying that the more UPy content in polyureas leads to more energy dissipation. These results confirm that the force-induced rupture of quadruple hydrogen bonds serving as additional sacrificial bonds contributes to more effective energy dissipation for PU-1/6UPy and PU-1/3UPy than that for PU-0UPy.

Quantitative analysis can straightforwardly determine the influence of UPy content on energy dissipation. We choose one typical cycle of PU-0UPy to explain the equation for calculating “energy loss coefficient” in Fig. S7 (in ESI). The integrated area of hysteresis loop is defined as “dissipated work density”, while “energy loss coefficient” can be obtained from dividing the dissipated work density by the total work density.^[20] These data provide insight into the strain dependence of hysteresis loops. As presented in Fig. 7, at a slight strain (5%), the “energy loss coefficient” is almost the same, which is attributed to the molecular chain friction according to the step-wise energy dissipation mechanism reported by Xie *et al.*^[44] When the strain becomes larger (10%–30%), multi-dissipation mechanisms would play roles during tensile tests, including molecular chain friction and hydrogen bonds. At the same strain, the “energy loss coefficient” increases with increasing UPy mole fraction, which verifies the contribution of quadruple hydrogen bonds to energy dissipation because more energy is needed to break the

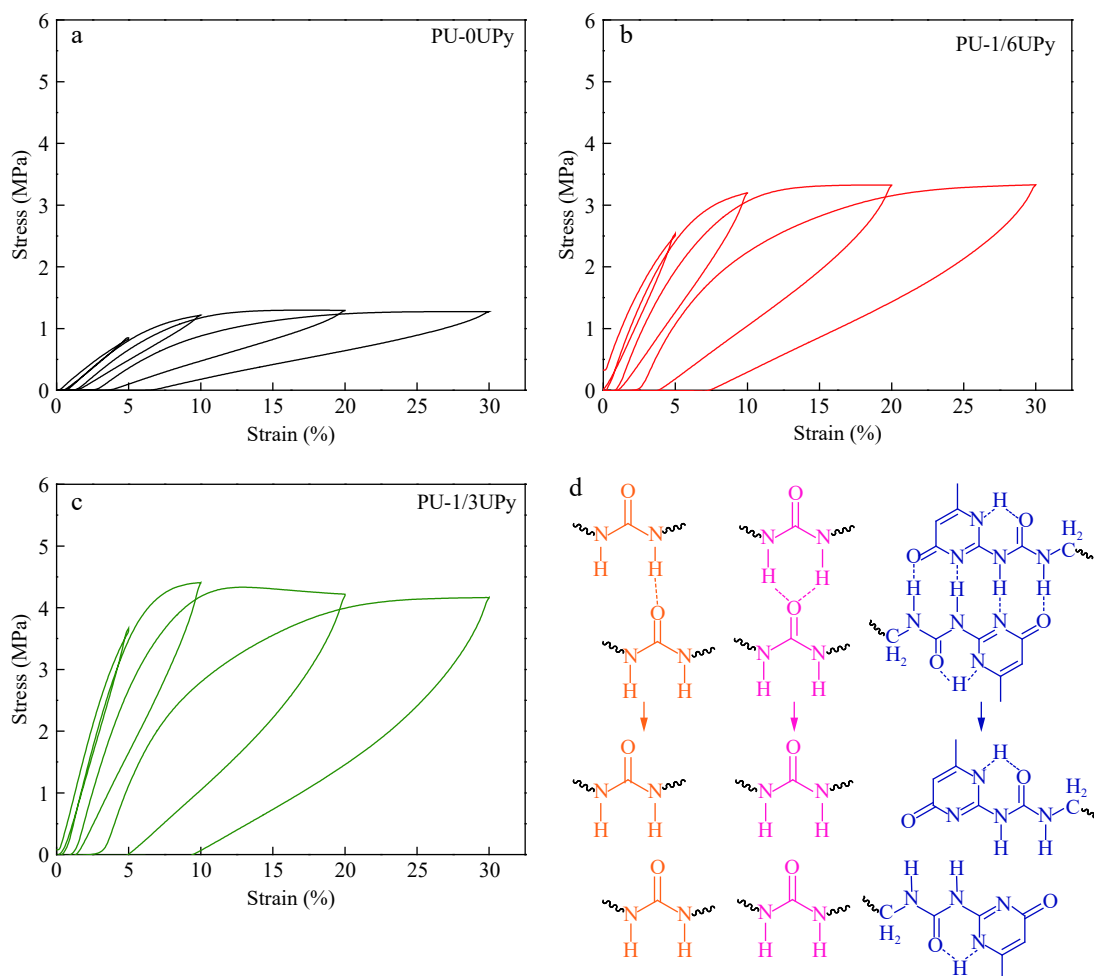


Fig. 6 Multiple consecutive incremental loading-unloading cycles of (a) PU-0UPy, (b) PU-1/6UPy, and (c) PU-1/3UPy; (d) Breakage of different hydrogen bonds

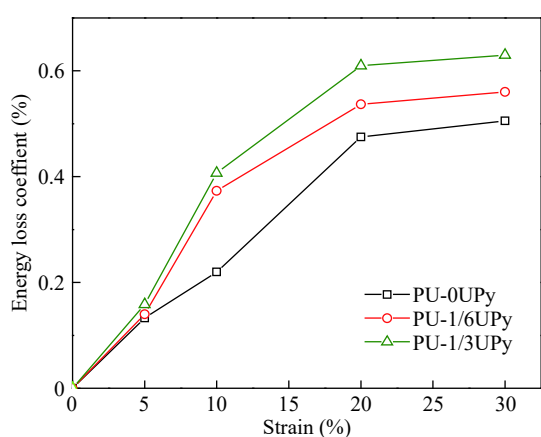


Fig. 7 Energy loss coefficients of different samples during the courses of loading-unloading

high energy quadruple hydrogen bonds. With strain increasing, the “energy loss coefficient” becomes larger, which indicates the continuous energy dissipation. Thus, we can deduce that the quadruple hydrogen bonding in hard segments prominently provides more energy dissipation due to the higher bond energy, affording toughened polyureas that can

find wider applications.

Effect of UPy Units on Soft Segmental Dynamics

Because the mobility of soft segments can influence the mechanical properties of polyureas^[41] and reflect the intermolecular forces of hard segments, the change in soft segmental dynamics of the three polyureas was investigated by measuring glass transition temperature (T_g) and the maximum relaxation time (τ_{max}) of soft segments, the two important parameters characterizing soft segmental dynamics. T_g s were obtained from both DMA and DSC (Figs. 8a and 8b), showing the same trend. It increased with increasing incorporation of UPy units, revealing slower soft segmental motion.

τ_{max} s of the three polyureas were measured by broadband dielectric spectrometer (BDS).^[42,43] In this work, a broad frequency and temperature range was chosen. ϵ'' as a function of frequency at different temperatures for PU-1/3UPy is shown in Fig. 8(c) as a representative. The loss peaks reflect α relaxation of the soft segments, shifting to higher frequency with increasing temperature.^[45] To systematically investigate the soft segmental dynamics, HN and VFT equations were utilized to describe the temperature dependence of

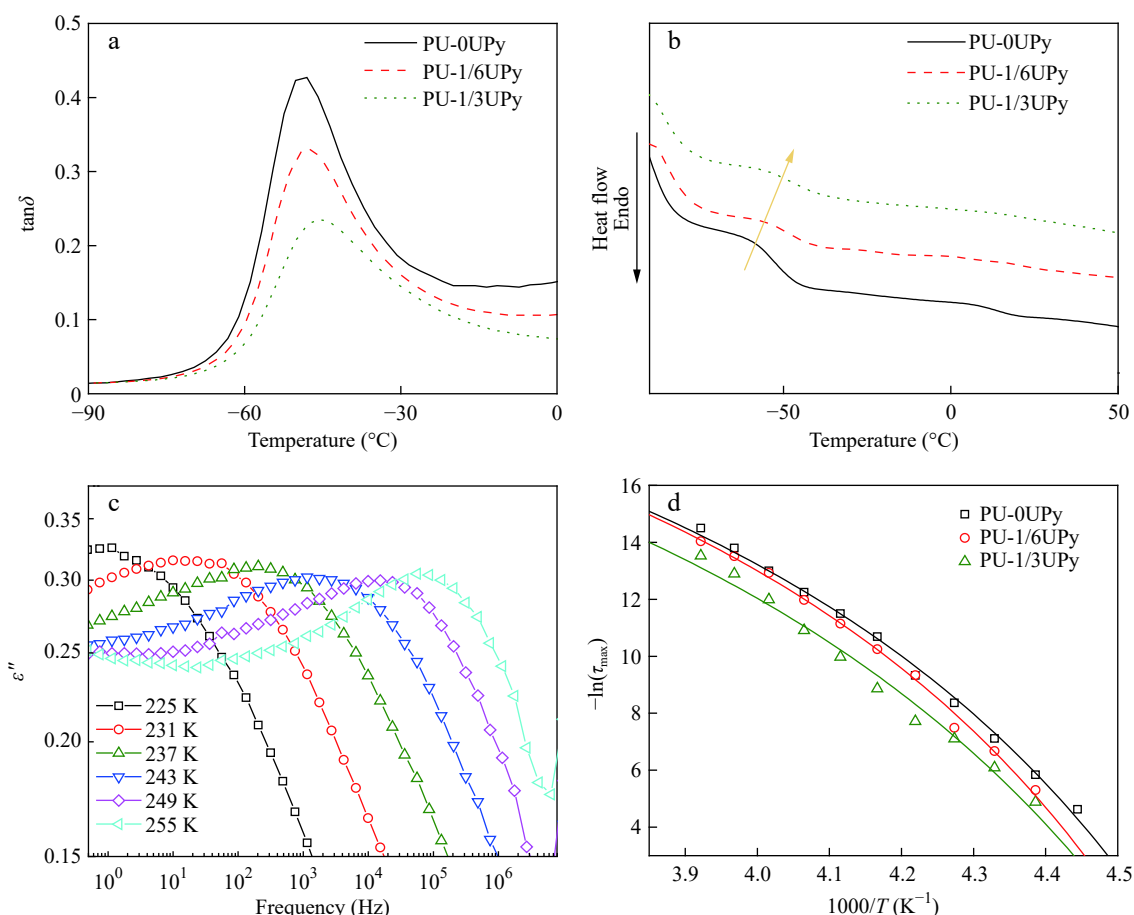


Fig. 8 (a) $\tan\delta$ measured by DMA, (b) DSC curves of different polyureas, (c) ε'' as a function of frequency for PU-1/3UPy, and (d) temperature dependence of τ_{\max} for segmental mode (Solid lines represent the VFT fitting curves.)

τ_{\max} in Fig. 8(d). τ_{\max} increased with increasing UPy content, which elucidates the restriction of UPy units on soft segments. Because the hard and soft segments were directly linked with each other *via* covalent bonds, the changes of the hard segment structure would influence the soft segments. When the hydrogen bonds became stronger, the motion of the soft segments would be hindered to some extent.

On the basis of the above discussion, both T_g and τ_{\max} indicate slower soft segmental dynamics after incorporation of UPy units. This should contribute not only to the enhancements of modulus and strength but also to the improvement of toughness as the chain friction increases.^[41]

CONCLUSIONS

The preparation of polyureas by replacing a portion of a classical diisocyanate with a UPy-derived diisocyanate is a well-defined quadruple hydrogen bonding strategy to promote the overall mechanical properties of polyureas through dimerization of UPy units. The Young's modulus, tensile strength, and toughness of the polyurea containing 1/6 molar fraction of UPy-derived diisocyanate were *ca.* 3.5, 3, and 5 times those of the polyurea without UPy, respectively. The high bonding energy of the quadruple hydrogen bonds of UPy dimers was the predominant molecular mechanism behind

the simultaneous stiffening, strengthening, and toughening effects. On the one hand, it makes the intermolecular forces among hard segments stronger. Since hard domains act as reinforcing fillers in polyureas, more rigid fillers result in the better stiffening and strengthening effects. On the other hand, more efficient energy dissipation associated with the breakage of stronger quadruple hydrogen bonds upon sample deformation leads to strong toughening effect. This work can provide an effective approach to comprehensively improve the mechanical properties of polyureas.

Electronic Supplementary Information

Electronic supplementary information (ESI) is available free of charge in the online version of this article at <http://dx.doi.org/10.1007/s10118-019-2275-3>.

ACKNOWLEDGMENTS

This work was financially supported by the National Natural Science Foundation of China (Nos. 51673110 and 51473085), the Joint Funds of the National Natural Science Foundation of China (No. U1862205), and Tsinghua University-Suzhou Innovation

Leading Program (No. 2016SZ0315).

REFERENCES

- Roland, C. M.; Twigg, J. N.; Vu, Y.; Mott, P. H. High strain rate mechanical behavior of polyurea. *Polymer* **2007**, *48*, 574–578.
- Sarva, S. Stress-strain behavior of a polyurea and a polyurethane from low to high strain rates. *Polymer* **2007**, *48*, 2208–2213.
- Yi, J. Large deformation rate-dependent stress-strain behavior of polyurea and polyurethanes. *Polymer* **2006**, *47*, 319–329.
- Choi, T.; Fragiadakis, D.; Roland, C. M.; Runt, J. Microstructure and segmental dynamics of polyurea under uniaxial deformation. *Macromolecules* **2012**, *45*, 3581–3589.
- Li, T.; Xie, Z.; Xu, J.; Weng, Y.; Guo, B. H. Design of a self-healing cross-linked polyurea with dynamic cross-links based on disulfide bonds and hydrogen bonding. *Eur. Polym. J.* **2018**, *107*, 249–257.
- Rinaldi, R. G.; Boyce, M. C.; Weigand, S. J.; Londono, D. J.; Guise, M. W. Microstructure evolution during tensile loading histories of a polyurea. *J. Polym. Sci., Part B: Polym. Phys.* **2011**, *49*, 1660–1671.
- Castagna, A. M.; Pangon, A.; Dillon, G. P.; Runt, J. Effect of thermal history on the microstructure of a poly(tetramethylene oxide)-based polyurea. *Macromolecules* **2013**, *46*, 6520–6527.
- Chao, L.; Ma, C.; Xie, Q.; Zhang, G. Self-repairing silicone coating for marine anti-biofouling. *J. Mater. Chem. A* **2017**, *5*, 15855–15861.
- Engels, H. W.; Pirkel, H. G.; Albers, R.; Albach, R. W.; Krause, J.; Hoffmann, A.; Casselmann, H.; Dormish, J. Polyurethanes: Versatile materials and sustainable problem solvers for today's challenges. *Angew. Chem. Int. Ed.* **2013**, *52*, 9422–9441.
- Frangiadakis, D.; Gamache, R.; Bogoslovov, R. B.; Roland, C. M. Segmental dynamics of polyurea: Effect of stoichiometry. *Polymer* **2010**, *51*, 178–184.
- Xuan, L.; Kuang, W.; Guo, B. Preparation of rubber/graphene oxide composites with *in situ* interfacial design. *Polymer* **2015**, *56*, 553–562.
- Qiao, H.; Wang, R.; Yao, H.; Zhou, X.; Lei, W.; Hu, X.; Zhang, L. Preparation of graphene oxide/bio-based elastomer nanocomposites through polymer design and interface tailoring. *Polym. Chem.* **2015**, *6*, 6140–6151.
- Qian, X.; Song, L.; Yu, B.; Yang, W.; Wang, B.; Hu, Y.; Yuen, R. K. One-pot surface functionalization and reduction of graphene oxide with long-chain molecules: Preparation and its enhancement on the thermal and mechanical properties of polyurea. *Chem. Eng. J.* **2014**, *236*, 233–241.
- Qian, X.; Song, L.; Tai, Q.; Hu, Y.; Yuen, R. K. Graphite oxide/polyurea and graphene/polyurea nanocomposites: A comparative investigation on properties reinforcements and mechanism. *Compos. Sci. Technol.* **2013**, *74*, 228–234.
- Wu, C.; Zhang, M. Q.; Rong, M. Z.; Friedrich, K. Silica nanoparticles filled polypropylene: Effects of particle surface treatment, matrix ductility and particle species on mechanical performance of the composites. *Compos. Sci. Technol.* **2005**, *65*, 635–645.
- Sánchez-Ferrer, A.; Rogez, D.; Martinoty, P. Synthesis and characterization of new polyurea elastomers by sol/gel chemistry. *Macromol. Chem. Phys.* **2010**, *211*, 1712–1721.
- Bras, W.; Derbyshire, G. E.; Bogg, D.; Cooke, J.; Elwell, M. J.; Komanschek, B. U.; Naylor, S.; Ryan, A. J. Simultaneous studies of reaction-kinetics and structure development in polymer processing. *Science* **1995**, *267*, 996–999.
- Elwell, M. J.; Ryan, A. J.; Grünbauer, H. J. M.; Lieshout, H. C. V. *In situ* studies of structure development during the reactive processing of model flexible polyurethane foam systems using FTIR spectroscopy, synchrotron SAXS, and rheology. *Macromolecules* **1996**, *212*, 2960–2968.
- Sami, S.; Yildirim, E.; Yurtsever, M.; Yurtsever, E.; Yilgor, E.; Yilgor, I.; Wilkes, G. L. Understanding the influence of hydrogen bonding and diisocyanate symmetry on the morphology and properties of segmented polyurethanes and polyureas: Computational and experimental study. *Polymer* **2014**, *55*, 4563–4576.
- Das, S.; Cox, D. F.; Wilkes, G. L.; Klinedinst, D. B.; Yilgor, I.; Yilgor, E.; Beyer, F. L. Effect of symmetry and H-bond strength of hard segments on the structure-property relationships of segmented, nonchain extended polyurethanes and polyureas. *J. Polym. Sci., Part B: Polym. Phys.* **2007**, *46*, 853–875.
- Das, S.; Yilgor, I.; Yilgor, E.; Wilkes, G. L. Probing the urea hard domain connectivity in segmented, non-chain extended polyureas using hydrogen-bond screening agents. *Polymer* **2008**, *49*, 174–179.
- Aneja, A.; Wilkes, G. L. Exploring macro-and microlevel connectivity of the urea phase in slabstock flexible polyurethane foam formulations using lithium chloride as a probe. *Polymer* **2002**, *43*, 5551–5561.
- Mattia, J.; Painter, P. A comparison of hydrogen bonding and order in a polyurethane and poly(urethane-urea) and their blends with poly(ethylene glycol). *Macromolecules* **2007**, *40*, 1546–1554.
- Appel, W. P. J.; Portale, G.; Wisse, E.; Dankers, P. Y. W.; Meijer, E. W. Aggregation of ureido-pyrimidinone supramolecular thermoplastic elastomers into nanofibers: A kinetic analysis. *Macromolecules* **2011**, *44*, 6776–6784.
- Cheng, C. C.; Yen, Y. C.; Chang, F. C. Self-supporting polymer from a POSS derivative. *Macromol. Rapid Commun.* **2011**, *32*, 927–932.
- Söntjens, S. H. M.; Renken, R. A. E.; Gemert, G. M. L. V.; Engels, T. A. P.; Bosman, A. W.; Janssen, H. M.; Govaert, L. E.; Baaijens, F. P. T. Thermoplastic elastomers based on strong and well-defined hydrogen-bonding interactions. *Macromolecules* **2008**, *41*, 5703–5708.
- Gooch, A.; Nedolisa, C.; Houton, K. A.; Lindsay, C. I.; Saiani, A.; Wilson, A. J. Tunable self-assembled elastomers using triply hydrogen-bonded arrays. *Macromolecules* **2012**, *45*, 4723–4729.
- Dankers, P. Y. W.; Zhang, Z.; Wisse, E.; Grijpma, D. W.; Sijbesma, R. P.; Feijen, J.; Meijer, E. W. Oligo(trimethylene carbonate)-based supramolecular biomaterials. *Macromolecules* **2006**, *39*, 8763–8771.
- Hirschberg, J. H. K. K.; Beijer, F. H.; Aert, H. A. V.; Magusin, P. C. M. M.; Sijbesma, R. P.; Meijer, E. W. Supramolecular polymers from linear telechelic siloxanes with quadruple-hydrogen-bonded units. *Macromolecules* **1999**, *32*, 2696–2705.
- Yan, X.; Liu, Z.; Zhang, Q.; Lopez, J.; Wang, H.; Wu, H. C.; Niu, S.; Yan, H.; Wang, S.; Lei, T. Quadruple H-bonding cross-linked supramolecular polymeric materials as substrates for stretchable, anti-tearing, and self-healable thin film electrodes. *J. Am. Chem. Soc.* **2018**, *140*, 5280–5289.
- Song, Y.; Liu, Y.; Qi, T.; Li, G. L. Towards dynamic but super-tough healable polymers through biomimetic hierarchical hydrogen-bonding interactions. *Angew. Chem. Int. Ed.* **2018**, *57*,

- 13838–13842.
- 32 Luo, M. C.; Jian, Z.; Xuan, F.; Huang, G.; Wu, J. Toughening diene elastomers by strong hydrogen bond interactions. *Polymer* **2016**, *106*, 21–28.
- 33 Jie, L.; Tang, Z.; Jing, H.; Guo, B.; Huang, G. Promoted strain-induced-crystallization in synthetic *cis*-1,4-polyisoprene via constructing sacrificial bonds. *Polymer* **2016**, *97*, 580–588.
- 34 Havriliak, S.; Negami, S. A complex plane representation of dielectric and mechanical relaxation processes in some polymers. *Polymer* **1967**, *8*, 161–210.
- 35 Sontjens, S. H. M.; Sijbesma, R. P.; van Genderen, M. H. P.; Meijer, E. W. Stability and lifetime of quadruply hydrogen bonded 2-ureido-4[1*H*]-pyrimidinone dimers. *J. Am. Chem. Soc.* **2000**, *122*, 7487–7493.
- 36 Beijer, F. H.; Sijbesma, R. P.; Kooijman, H.; Spek, A. L.; Meijer, E. W. Strong dimerization of ureidopyrimidones via quadruple hydrogen bonding. *J. Am. Chem. Soc.* **1998**, *120*, 6761–6769.
- 37 Wei, M.; Zhan, M.; Yu, D.; Xie, H.; He, M.; Yang, K.; Wang, Y. Novel poly(tetramethylene ether)glycol and poly(ϵ -caprolactone) based dynamic network via quadruple hydrogen bonding with triple-shape effect and self-healing capacity. *ACS Appl. Mater. Interfaces* **2015**, *7*, 2585–2596.
- 38 Lai, Y.; Kuang, X.; Zhu, P.; Huang, M.; Dong, X.; Wang, D. Colorless, transparent, robust, and fast scratch-self-healing elastomers via a phase-locked dynamic bonds design. *Adv. Mater.* **2018**, *30*, 1802556.
- 39 Teo, L. S.; Chen, C. Y.; Kuo, J. F. Fourier transform infrared spectroscopy study on effects of temperature on hydrogen bonding in amine-containing polyurethanes and poly(urethane-urea)s. *Macromolecules* **1997**, *30*, 1793–1799.
- 40 Srichatrapimuk, V. W.; Cooper, S. L. Infrared thermal analysis of polyurethane block polymers. *J. Polym. Sci., Part B: Polym. Phys.* **1978**, *15*, 267–311.
- 41 Prisacariu, C. *Polyurethane elastomers: from morphology to mechanical aspects*. Springer Science & Business Media, **2011**.
- 42 Neal, J. A.; Mozhdzhi, D.; Guan, Z. Enhancing mechanical performance of a covalent self-healing material by sacrificial non-covalent bonds. *J. Am. Chem. Soc.* **2015**, *137*, 4846–4850.
- 43 Cordier, P.; Tournilhac, F.; Soulié-Ziakovic, C.; Leibler, L. Self-healing and thermoreversible rubber from supramolecular assembly. *Nature* **2008**, *451*, 977.
- 44 Liu, X. Y.; Ming, Z.; Shi, F. K.; Hao, X.; Xie, X. M. Multi-bond network hydrogels with robust mechanical and self-healable properties. *Chinese J. Polym. Sci.* **2017**, *35*, 1253–1267.
- 45 Luo, M. C.; Zhang, X. K.; Zeng, J.; Gao, X. X.; Huang, G. S. Enhanced relaxation behavior below glass transition temperature in diene elastomer with heterogeneous physical network. *Polymer* **2016**, *91*, 81–88.